JOURNAL OF BACTERIOLOGY, Nov. 2009, p. 6822–6832 Vol. 191, No. 22
0021-9193/09/$12.00 doi:10.1128/JB.00618-09

σ^X Is Involved in Controlling *Bacillus subtilis* Biofilm Architecture through the AbrB Homologue Abh[▽]

Ewan J. Murray,[1] Mark A. Strauch,[2] and Nicola R. Stanley-Wall[1]*

Division of Molecular Microbiology, College of Life Sciences, MSI/WTB/JBC Complex, University of Dundee, Dundee DD1 5EH, United Kingdom,[1] and Department of Microbial Pathogenesis, Dental School, University of Maryland, Baltimore, 650 W. Baltimore Street, Baltimore, Maryland 21201[2]

Received 12 May 2009/Accepted 3 September 2009

A characteristic feature of biofilm formation is the production of a protective extracellular polymeric matrix. In the gram-positive bacterium *Bacillus subtilis*, the biofilm matrix is synthesized by the products of the *epsABCDEFGHIJKLMNO* operon (hereafter called the *eps* operon) and *yqxM-sipW-tasA* loci. Transcription from these operons is repressed by two key regulators, AbrB and SinR. Relief of inhibition is necessary to allow biofilm formation to proceed. Here we present data indicating that Abh, a sequence and structural homologue of AbrB, regulates biofilm architecture by *B. subtilis* when colony morphology and pellicle formation are assessed. Data indicating that *abh* expression is dependent on the environmental signals that stimulate the activity of the extracytoplasmic function σ-factor σ^X are shown. We demonstrate that expression of *slrR*, the proposed activator of *yqxM* transcription, is positively controlled by Abh. Furthermore, Abh is shown to activate transcription from the promoter of the *eps* operon through its control of SlrR. These findings add to the increasingly complex transcriptional network that controls biofilm formation by *B. subtilis*.

Multicellular behaviors exhibited by microorganisms are survival strategies often associated with "stationary-phase" growth. The gram-positive soil-dwelling bacterium *Bacillus subtilis* is capable of many such behaviors, including cannibalism (16), genetic competence (19), exoprotease production (13), and biofilm formation (7, 20). If unfavorable conditions persist, *B. subtilis* is also capable of sporulation, a process that results in the formation of a dormant stress-resistant endospore (43). Both the processes of sporulation and biofilm formation are controlled in *B. subtilis* by the global regulator of multicellular behavior, Spo0A (7, 20, 43). Spo0A exhibits regulatory control when phosphorylated. Phosphorylation occurs through the action of a complex phosphorelay that is initiated in response to multiple environmental stimuli (9, 17). The promoter regions of Spo0A-regulated genes have been determined to possess different binding affinities for the activated regulator (15). Therefore, the impact of Spo0A~P is determined by the extent to which Spo0A~P accumulates within an individual cell. This simple but effective mechanism permits Spo0A~P to control multiple incompatible cell states (15, 55). For example, transcription of the genes required for biofilm formation is induced before transcription of the genes required for spore formation (55). In this case, formation of a biofilm could perhaps allow scarce nutrients to be shared among the community in the hope that environmental conditions would improve so that cells do not have to instigate the irreversible and energetically expensive sporulation pathway.

Biofilm formation by *B. subtilis* occurs upon activation of two transcription factors, Spo0A and DegU (34, 40). DegU activates transcription of *yvcA* and *yuaB*, but how the products of these loci contribute to the formation of a mature biofilm remains unknown (30, 53, 54). As discussed above, Spo0A is required for biofilm formation and its activation is triggered by the lipopeptide surfactin (7, 20, 33). Downstream from Spo0A are two parallel pathways of repression and antirepression (2). Transcription of the operons required for the synthesis of the extracellular matrix is repressed by two key regulators, namely, AbrB and SinR (21, 28). Spo0A~P-dependent derepression of both the AbrB and SinR regulons occurs by the induction of antagonist proteins that inhibit the ability of both repressors to bind DNA, namely, AbbA which interacts with AbrB, and SinI which interacts with SinR (1, 2). Spo0A~P also directly inhibits *abrB* transcription (15, 46, 51). Thus, deletion of either *abrB* or *sinR* results in increased extracellular matrix production and a more rugose biofilm (34).

A key feature of biofilm formation is the synthesis of the extracellular matrix and the inhibition of motility (3, 34, 48). To date, two components of the biofilm matrix formed by *B. subtilis* strain NCIB3610 have been described, an exopolysaccharide and a protein called TasA. The chemical composition of the exopolysaccharide remains undefined, but it is known that the machinery required for its synthesis is encoded by the 15-gene *epsABCDEFGHIJKLMNO* operon (hereafter called the *eps* operon) (7, 34). The molecular function of all but one of the products of the *eps* operon is unknown, but EpsE interacts with the flagellar motor to render the cells immotile during biofilm formation (3). TasA, the major protein component of *B. subtilis* biofilm is the product of a three-gene operon, the *yqxM-sipW-tasA* operon (hereafter called the *yqxM* operon). The *yqxM* operon additionally encodes the proteins required for the correct localization of TasA within the matrix of the biofilm (6, 11).

Abh is a sequence and structural homologue of AbrB with 70% identity in the DNA binding domain (5). Despite this, the

* Corresponding author. Mailing address: Division of Molecular Microbiology, College of Life Sciences, MSI/WTB/JBC Complex, University of Dundee, Dundee DD1 5EH, United Kingdom. Phone: 44(0)1382 386335. Fax: 44(0)1382 386375. E-mail: n.r.stanleywall@dundee.ac.uk.

▽ Published ahead of print on 18 September 2009.

physiological role of Abh has remained relatively unknown. Most information concerning Abh function is derived from a study by Strauch et al. (49) who identified the first set of genes regulated by Abh. The genes identified regulate the production of antimicrobial compounds. The genes identified as directly regulated by Abh were also shown to be directly regulated by AbrB, thereby suggesting a significant Abh and AbrB regulatory overlap (35, 49). Production of Abh is regulated at the level of transcription (27, 49). Expression of *abh* is directly repressed by AbrB, and consequently, genes that are regulated by Abh are also indirectly controlled by Spo0A~P (see above) (49). In addition, transcription of *abh* is activated by RNA polymerase in the presence of the *e*xtracytoplasmic *f*unction (ECF) σ-factors, σ^X (in vitro and in vivo data) and σ^W (in vitro data) (26, 27). More recently, by using a more stringent set of conditions, *abh* was also ascribed to the σ^M regulon (14). The *B. subtilis* genome encodes seven ECF σ-factors, six of which are "anchored" to the cytoplasmic membrane by their cotranscribed antagonist (32, 38, 58). Upon the sensing of a specific external stress, intramembrane proteolysis of the antagonist allows release of a specific σ-factor into the cytoplasm where it is free to interact with RNA polymerase and regulate their specific regulon (24).

Using an "undomesticated" isolate of *B. subtilis*, NCIB3610, we demonstrate that the AbrB homologue Abh regulates biofilm architecture. We show that the level of Abh synthesis is controlled by an unidentified environmental signal that stimulates the activity of the ECF σ-factor σ^X under biofilm formation conditions. Furthermore, we show that Abh regulates the activation of transcription from the *eps* operon which provides the extracellular polysaccharide component of the matrix and inhibits flagellum-based motility during biofilm formation (3, 7). It has previously been shown that biofilm formation requires the transcriptional activator SlrR (12, 31), and using single-cell analysis, we show that transcription of *slrR* is positively controlled by Abh. Consistent with this observation, the mutant biofilm generated in the absence of *abh* can be complemented by ectopic expression of *slrR*. Our data suggest that Abh indirectly activates biofilm formation via activation of *slrR*, which in turn increases the number of cells actively transcribing the genes required for synthesizing both the protein and polysaccharide components of the biofilm matrix.

MATERIALS AND METHODS

General strain construction and growth conditions. The *B. subtilis* strains used and constructed in this study are detailed in Table 1. *Escherichia coli* strain MC1061 [F′ *lacI*^{q} *lacZM15* Tn*10* (*tet*)] was used for the construction and maintenance of plasmids. *B. subtilis* JH642 and 168 derivatives were generated by transformation of competent cells with plasmids or DNA using standard protocols (22). SPP1 phage transductions, for introduction of DNA into *B. subtilis* strain NCIB3610, were conducted as described previously (53). Both *E. coli* and *B. subtilis* strains were routinely grown in Luria-Bertani (LB) medium (10 g NaCl, 5 g yeast extract, and 10 g tryptone [all per liter]) or MSgg medium (5 mM potassium phosphate and 100 mM morpholinepropanesulfonic acid [MOPS] at pH 7.0 supplemented with 2 mM $MgCl_2$, 700 μM $CaCl_2$, 50 μM $MnCl_2$, 50 μM $FeCl_3$, 1 μM $ZnCl_2$, 2 μM thiamine, 0.5% glycerol, 0.5% glutamate, and amino acids as appropriate at a final concentration of 50 μg ml^{-1}) at 37°C (7, 11). When appropriate, the following antibiotics and concentrations were used: ampicillin at 100 μg ml^{-1}), chloramphenicol at 5 μg ml^{-1}, erythromycin at 5 μg ml^{-1}, lincomycin at 25 μg ml^{-1}, kanamycin at 25 μg ml^{-1}, and spectinomycin at 100 μg ml^{-1}.

Strain construction. To delete *abh*, long-flanking homology PCR was used based on a method previously described (37). The region overlapping the translational start codon of *abh* was amplified using primers NSW504 (5′-CTGCGATCACGCCATCTTTCATCG-3′) and NSW505 (5′-*GTTATCCG CTCACAATT C*TGATTTCATAAAAACCCTTCTTCC-3′), and the region overlapping the termination stop codon of *abh* was amplified using primers NSW506 (5′-*CGTC GTGACTGGGAAAC*AAAGAATAAAATTATGCTAAAAAAGGC-3′) and NSW510 (5′-CGATTTCCTGCAAATTATCCAATGATGCGG-3′). The translational start codon is indicated by a single underline, and the translational termination codon is indicated by double underline. Sequences in italics are homologous to the primer sequences used to amplify the chloramphenicol resistance gene. The chloramphenicol resistance gene was amplified from plasmid pCBB31 using primers NSW107 (5′-GTTTTCCCAGTCACGACG-3′) and NSW108 (5′-GAATTGTGAGCGGATAAC-3′). The purified fragments were combined in a PCR using primers NSW504 and NSW510 using LA *Taq* (TaKaRa). The fragment generated was transformed into *B. subtilis* JH642, and the resulting colonies were screened by PCR to ensure double recombination at the *abh* locus (NRS1894 Δ*abh*::*cat*). The mutated *abh* gene was transferred to strain NCIB3610 by phage transduction, selecting for chloramphenicol resistance (strain NRS1900).

Plasmid construction. Plasmid pBL154 was used to complement the Δ*abh* strain by ectopic expression at the *amyE* locus using its native promoter. The *abh* coding region plus 172 bp of the upstream region was PCR amplified using primers BL189 (5′-GCGCGGATCCCAAGGAACTGTGTGTAAC-3′) and BL198 (5′-GCGCGAATTCTTATTCTTTTAAAGCGGC-3′) and ligated into pDG1730 (18) at the BamHI and EcoRI restriction sites. Ectopic expression of *abh* at *amyE* was placed under the control of two separate isopropyl-β-D-thiogalactopyranoside (IPTG)-inducible promoters $P_{hy\text{-}spank}$ and $P_{hy\text{-}spac}$ using plasmid backbones pDR111 (8) and pPL82 (44), respectively. Plasmids pNW400 (pDR111 derived) and pNW403 (pPL82 derived) were generated by amplification of the *abh* coding region and the native ribosome binding site using primers NSW502 (5′-CGTAAAGCTTGGAAGAAGGGTTTTTATGAAATCAATAG GTGTT-3′) and NSW503 (5′-CGTAGCATGCTTATTCTTTTAAAGCGGCT TG-3′). PCR products were ligated into pDR111 and pPL82 at the HindIII and SphI restriction sites. Plasmid pNW402 was used to assay *abh* expression utilizing green fluorescent protein (GFP) production as a reporter that was driven by the upstream promoter region of *abh* (−500 bp relative to the A nucleotide of the *abh* translational start codon). The promoter region was amplified using primer pair NSW521 (5′-GCTAGAATTCCTGCGATCACGCCATCTTTCA-3′) and NSW522 (5′-CGTAAAGCTTAAAAACCCTTCTTCCTTTAAA-3′) and ligated into pBL165 using the EcoRI and HindIII sites (48). Plasmid pNW408 was constructed by PCR amplification of the upstream region of the *slrR* gene as defined by Chu et al. (12) using primer pair NSW710 (5′-GTCGAATTCCTAG ACAATCGCATATAA TTCTTTG-3′) and NSW711 (5′-GTCAAGCTTCTAG AAATTCTCCTCTATTCCTGTCG-3′). The amplified fragment was cloned into vector pMF302 (15) at the EcoRI and HindIII restriction sites. The newly constructed plasmid was digested with EcoRI and BamHI to release the P*slr-gfp* fragment that was ligated into pSac-Kan to allow integration at the *sacA* locus (39). Plasmid pNW602 was used to assay *yqxM* expression utilizing GFP production as a reporter that was driven by the upstream region of *yqxM* (−490 bp relative to the A nucleotide of the *yqxM* translational start codon). The promoter region was amplified using primers NSW620 (5′-GATGAATTCTCAAGTTAA ATGGTATTGAT-3′) and NSW621 (5′-GATAAGCTTGTAAAACACTGTAA CTTG-3′) and ligated into pBL165 using the EcoRI and HindIII sites (48) to generate pNW600. pNW600 was then digested with EcoRI and BamHI to release the P_{yqxM}-*gfp* fragment that was ligated into pSac-Kan to allow integration at the *sacA* locus (39). Plasmid pNW502 was used to assay *epsA* expression utilizing GFP production as a reporter that was driven by the upstream region of *epsA* (−300 bp relative to the A nucleotide of the *epsA* translational start codon). The promoter region was amplified using primers NSW618 (5′-GTCGAATTC GAAATTCTCCTCTAATCCTG-3′) and NSW619 (5′-GATAAGCTTCATAG CCTTCAGCCTT-3′) and ligated into pBL165 using the EcoRI and HindIII sites (48) to generate pNW501. pNW501 was then digested with EcoRI and BamHI to release the P_{epsA}-*gfp* fragment that was cloned into pSac-Kan to allow integration at the *sacA* locus (39). Plasmid pNW407 was used to induce *slrR* expression in an IPTG-dependent manner. Primers slrR-F (5′-CGTAAAGCTTAGA GGAGAATTTCATATTATGATTGGAAGAATTATCCG-3′) and slrR-R (5′-AAAAGCATGCTCATCTTCCCTTTGTTTTTAAAAAGGATTTG ACTTCA TG-3′) were used to amplify the *slrR* gene and its native ribosome binding site. The PCR product was ligated into pDR111 (8) at the HindIII and SphI restriction sites. All plasmids generated were sequenced to ensure the absence of PCR-incorporated sequence errors.

Flow cytometry. The fluorescence of strains harboring GFP promoter fusions was measured in biofilm-forming conditions after 18 h of incubation at 37°C using the previously described method (55). Single-cell fluorescence was directly measured on a BD FACSCalibur (BD Biosciences). Single cells were identified

TABLE 1. Strains used in this study

Strain	Relevant genotype or description[a]	Source or construction[b]
168	*trpC2*	BGSC
HB0801	*sigM*::*kan*	36
HB0803	*sigW*::*mls*	36
HB0804	*sigX*::*spc*	36
JH642	*trpC2 pheA1*	42
NCIB3610	Prototroph	BGSC
NRS1314	*degU*::pBL204 (*cat*)	53
NRS1434	*trpC2 pheA1 amyE*::P_{abh}-*abh*::*spc*	pBL154 → JH642
NRS1893	*trpC2 pheA1 amyE*::$P_{hy\text{-}spank}$-*abh-lacI* (*spc*)	pNW400 → JH642
NRS1894	*trpC2 pheA1* Δ*abh*::*cat*	This study
NRS1900	Δ*abh*::*cat*	SPP1 NRS1894 → NCIB3610
NRS1901	Δ*abh*::*cat amyE*::$P_{hy\text{-}spank}$-*abh-lacI* (*spc*)	SPP1 NRS1893 → NRS1900
NRS1904	Δ*abh*::*cat amyE*::P_{abh}-*abh*::*spc*	SPP1 NRS1434 → NRS1900
NRS1916	*trpC2 pheA1 amyE*::P_{abh}-*gfp* (*cat*)	pNW402 → JH642
NRS1917	*amyE*::P_{abh}-*gfp* (*cat*)	SPP1 NRS1916 → NCIB3610
NRS1937	*trpC2 pheA1 amyE*::$P_{hy\text{-}spac}$-*abh-lacI* (*cat*)	pNW403 → JH642
NRS1964	*trpC2 pheA1 amyE*::$P_{hy\text{-}spank}$ *slrR-lacI* (*spc*)	pNW407 → JH642
NRS1965	*amyE*::$P_{hy\text{-}spank}$-*slrR-lacI* (*spc*)	SPP1 NRS1964 → NCIB3610
NRS1966	Δ*abh*::*cat amyE*::$P_{hy\text{-}spank}$ *slrR-lacI* (*spc*)	SPP1 NRS1964 → 1900
NRS1968	*trpC2 sacA*::P_{slrR}-*gfp-lacI* (*kan*)	pNW408 → 168
NRS2241	*trp*C2 *pheA1 sacA*::P_{epsA}-*gfp* (*kan*)	pNW502 → JH642
NRS2242	*sacA*::P_{epsA}-*gfp* (*kan*)	SPP1 NRS2241 → NCIB3610
NRS2388	*trpC2 sacA*::P_{yqxM}-*gfp* (*kan*)	pNW602 → 168
NRS2394	*sacA*::P_{yqxM}-*gfp* (*kan*)	SPP1 NRS2388 → NCIB3610
NRS2547	Δ*abh*::*cat sacA*::P_{epsA}-*gfp* (*kan*)	SPP1 NRS1894 → NRS2242
NRS2549	Δ*abh*::*cat sacA*::P_{yqxM}-*gfp* (*kan*)	SPP1 NRS1894 → NRS2394
NRS2550	*sacA*::P_{slrR}-*gfp-lacI* (*kan*)	SPP1 NRS1968 → NCIB3610
NRS2551	Δ*abh*::*cat sacA*::P_{slrR}-*gfp-lacI* (*kan*)	SPP1 NRS1968 → NRS1900
NRS2552	Δ*abh*::*cat amyE*::$P_{hy\text{-}spank}$-*abh-lacI* (*spc*) *sacA*::P_{slrR}-*gfp-lacI* (*kan*)	SPP1 NRS1968 → NRS1901
NRS2553	Δ*abh*::*cat amyE*::P_{abh}-*abh*::*spc sacA*::P_{slrR}-*gfp-lacI* (*kan*)	SPP1 NRS1968 → NRS1904
NRS2556	Δ*abh*::*cat amyE*::P_{abh}-*abh*::*spc sacA*::P_{epsA}-*gfp* (*kan*)	SPP1 NRS1434 → NRS2547
NRS2557	Δ*abh*::*cat amyE*::P_{abh}-*abh*::*spc sacA*::P_{yqxM}-*gfp* (*kan*)	SPP1 NRS1434 → NRS2549
NRS2562	*amyE*::$P_{hy\text{-}spank}$-*slrR-lacI sacA*::P_{yqxM}-*gfp* (*kan*)	SPP1 NRS1964 → NRS2394
NRS2566	*amyE*::$P_{hy\text{-}spank}$-*slrR-lacI sacA*::P_{slrR}-*gfp* (*kan*)	SPP1 NRS1964 → NRS2550
NRS2571	*sigW*::*mls*	SPP1 HB0803 → NCIB3610
NRS2572	*sigX*::*spc*	SPP1 HB0804 → NCIB3610
NRS2574	*sigW*::*mls amyE*::$P_{hy\text{-}spac}$-*abh-lacI* (*cat*)	SPP1 NRS1937 → NRS2571
NRS2575	*sigX*::*spc amyE*::$P_{hy\text{-}spac}$-*abh-lacI* (*cat*)	SPP1 NRS1937 → NRS2572
NRS2576	*sigM*::*kan amyE*::P_{abh}-*gfp* (*cat*)	SPP1 NRS1916 → NRS2570
NRS2577	*sigX*::*spc amyE*::P_{abh}-*gfp* (*cat*)	SPP1 NRS1916 → NRS2572
NRS2578	*sigW*::*mls amyE*::P_{abh}-*gfp* (*cat*)	SPP1 NRS1916 → NRS2571
NRS2605	Δ*abh*::*cat amyE*::$P_{hy\text{-}spank}$-*slrR-lacI* (*spc*) *sacA*::P_{epsA}-*gfp* (*kan*)	SPP1 NRS1964 → NRS2547
NRS2606	Δ*abh*::*cat amyE*::$P_{hy\text{-}spank}$-*slrR-lacI* (*spc*) *sacA*::P_{yqxM}-*gfp*(*kan*)	SPP1 NRS1964 → NRS2549
NRS2716	*degU*::pBL204 (*cat*) *sacA*::P_{slrR}-*gfp-lacI* (*kan*)	SPP1 NRS1314 → NRS2550

[a] Drug resistance cassettes are indicated as follows: *cat*, chloramphenicol resistance; *kan*, kanamycin resistance; *mls*, lincomycin-erythromycin resistance; *spc*, spectinomycin resistance.

[b] The direction of strain construction is indicated with DNA or phage (SPP1) (→) recipient strain. BGSC is the *Bacillus* Genetic Stock Center.

on the basis of forward and side scatter, while GFP fluorescence was analyzed using 488 nm excitation with detection at 530 ± 30 nm. Data were captured using Cell Quest Pro (BD Biosciences) and further analyzed using FlowJo software version 4.3. For data profiles that gave a normal distribution, the geometric mean fluorescence was used as a measure of gene expression. The final fluorescence value was generated by subtraction of the geometric mean generated for the autofluorescence of each strain's nonfluorescent parent. The number of GFP-positive cells was calculated as the number of cells that exhibited a fluorescence signal greater than that generated by their nonfluorescent parent.

Biofilm formation conditions and image analysis. Biofilms were grown as described previously (7). After either 18 or 40 h of growth at 37°C, biofilm images were captured using a Leica MZ16 FA stereoscope using LAS software version 2.7.1. Scale bars depicted on each figure as a white or black bar represent the distance of 5 mm. Air-surface interface biofilms called pellicles were formed as described previously (7).

DNA footprinting analysis. Purification of Abh and AbrB was conducted as previously described (49). The DNA fragment used in DNase I footprinting assays was the following: an EcoRI-HindIII fragment of approximately 350 bp (containing the *slrR* and *epsA* promoter regions) was amplified using primers NSW737 (5′-CGTGAATTCCAGCACGAATCTGTG-3′) and NSW739 (5′-CGTAAGCTTCAGCTGATTAATAGA-3′) from the chromosome of strain NCIB3610 and cloned into pUC19 to yield pNW420. The plasmid containing the fragment was linearized at a unique restriction enzyme site flanking the insert and labeled using [α-^{32}P]dATP (Amersham) and the Klenow enzyme, followed by inactivation of the Klenow enzyme and the release of the singly end-labeled fragment via digestion at a unique site on its opposite flank. Labeled DNA fragments were purified using standard polyacrylamide gel electrophoresis and electroelution techniques. Protein binding buffer composition (1×) was 50 mM Tris (either pH 7 or pH 8), 10 mM $MgCl_2$, 100 mM KCl, 10 mM 2-mercaptoethanol, and 100 μg/ml bovine serum albumin. We have previously determined that optimal Abh binding affinity occurs at pH 7 in vitro, whereas optimal AbrB affinity occurs in a broad plateau from pH 8 to above pH 9.5, with only a slight decrease (about twofold) seen for binding at pH 7 (5). Therefore, we performed the in vitro DNA binding reactions using AbrB at pH 8 and the Abh reactions at both pH 7 and pH 8. DNase I footprinting assays were performed at room temperature (22°C) and analyzed as described previously (50, 57).

Electrophoretic mobility shift assay (EMSA). The binding conditions and target DNA were as described above for the footprinting analysis. Binding was

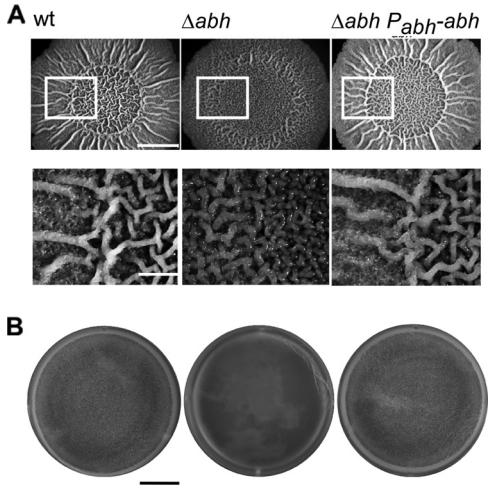

FIG. 1. Abh controls biofilm architecture. (A) Representative images showing biofilm architecture after 40 h of growth at 37°C on MSgg medium. The wild-type (wt) strain (NCIB3610), Δ*abh* (NRS1900), and Δ*abh*+P_{abh}-*abh* (NRS1904) strains are shown. Bars, 5 mm (top images) and 1.25 mm (bottom images). (B) Pellicle morphology after 18 h growth at 37°C in MSgg medium. The wild-type (wt) strain (NCIB3610), Δ*abh* (NRS1900), and Δ*abh*+P_{abh}-*abh* (NRS1904) strains are shown. Bar, 8 mm.

allowed to proceed for 15 min at room temperature, and the reaction mixtures were loaded onto 6% polyacrylamide gels (1× Tris-borate-EDTA [TBE] buffer). After electrophoresis, the gels were dried, imaged using an Amersham Typhoon 9000 phosphorimager, and quantitated using ImageQuant software.

RESULTS AND DISCUSSION

Abh controls *B. subtilis* biofilm architecture. We initiated this study with the aim of investigating whether the paralogue of the biofilm inhibitor AbrB (12, 21) Abh controlled biofilm formation based upon the knowledge that Abh and AbrB share an overlapping regulon (35, 49). We used rugose colony morphology and the formation of an air/surface interface biofilm called a pellicle as two independent indicators of biofilm formation (7). These types of biofilms have been shown to depend on the biosynthesis of the extracellular matrix (7, 55). All of our studies have been conducted using the undomesticated strain NCIB3610, as it forms more robust biofilms by comparison with isolates derived from the domesticated strain 168 (7). The morphologies of biofilms formed in the presence and absence of Abh are shown in Fig. 1. These images clearly show that the Δ*abh* strain (NRS1900) displays reduced biofilm architecture by comparison to the wild-type strain. This can be complemented by ectopic expression of *abh* under the control of its own promoter (NRS1904). The alteration in biofilm formation is apparent in both the colony assay (Fig. 1A) and the pellicle assay (Fig. 1B). Additionally, deletion of *abh* from the domesticated *B. subtilis* strain, JH642, resulted in a threefold decrease in biofilm formation as measured using a crystal violet-based biofilm microtiter plate assay (data not shown). Further evidence to support our conclusion that Abh positively controls biofilm formation was generated as part of a systematic analysis of all known transcriptional regulators of *B. subtilis* strain ATCC 6051 (29). The impact of deletion on pellicle formation was assessed, and Abh was shown to promote pellicle formation by *B. subtilis* strain ATCC 6051 (29). In toto, we conclude that Abh is required for the formation of a wild-type biofilm by *B. subtilis*.

σ^X activates *abh* expression. We were interested in establishing how transcription of *abh* was controlled under biofilm formation conditions. Using both in vitro and in vivo techniques, *abh* expression has previously been shown to be transcribed by the RNA polymerase core enzyme in the presence of the extracytoplasmic function sigma factor σ^X (26, 27). In vitro analysis also indicates that σ^W can activate *abh* transcription, although this has not been determined in vivo (26). More recently, it was proposed that *abh* transcription is activated by σ^M (14), raising the number of ECFs potentially responsible for *abh* transcription in vivo to three. We wanted to test which one of σ^X, σ^W, or σ^M had the dominant role in regulating *abh* transcription under biofilm formation conditions in the undomesticated strain NCIB3610. To do this, a P_{abh}-*gfp* reporter construct was generated (pNW402) and introduced into the wild-type NCIB3610 (NRS1917). The level of *abh* expression was measured in vivo during biofilm formation for each of the individual σ-factor mutants (σ^M, σ^W, and σ^X mutants) using flow cytometry. To compensate for any differences in background fluorescence, each strain carrying the P_{abh}-*gfp* construct was analyzed at the same time as a parent strain lacking the transcriptional fusion (see Materials and Methods). This ensured that the changes in fluorescence which were measured were not a result of changes in cell shape or some other phenotype. It was determined that P_{abh}-*gfp* displayed a narrow unimodal Gaussian distribution, indicative of transcription in all cells within the biofilm population (Fig. 2A). As P_{abh}-*gfp* expression followed a normal distribution, the geometric mean of the fluorescence value of the population of cells was used directly as a measure of gene expression. The expression of P_{abh}-*gfp* is σ^X dependent during biofilm formation, with ca. 18-fold reduction ($P < 0.01$) in P_{abh}-*gfp* expression being measured in the σ^X mutant by comparison with the wild type (Fig. 2B). The data also indicate that there is a small reduction in the level of *abh* transcription in the σ^W mutant while the σ^M mutant displays wild-type P_{abh}-*gfp* expression levels (Fig. 2B). These findings are slightly different from a recent study conducted using a laboratory isolate of *B. subtilis* where only upon deletion of both the σ^X and σ^M mutant genes was a large reduction in *abh* transcription observed (35). This highlights the strain-specific differences that exist between undomesticated and domesticated strains of *B. subtilis* and the value of analyzing different isolates of the same bacterial species.

Artificial induction of *abh* transcription in the σ^X mutant restores wild-type biofilm architecture. In good agreement with the observation that the σ^X mutant has a low level of *abh* transcription, the σ^X mutant displayed a reduction in the complexity of biofilm architecture that was comparable to that of the Δ*abh* strain (Fig. 2C). Both the *abh* and σ^X mutant strains fail to develop the complex "raised bundles" and "veins" seen to develop in the wild type. Additionally, unlike the wild-type strain, the σ^X mutant was unable to from a robust and rugose pellicle (Fig. 2D). In contrast, the σ^M and σ^W mutants that had wild-type levels of *abh* transcription also displayed wild-type biofilm architecture and formed a rugose pellicle (data not shown). To confirm that the reduction in biofilm complexity observed in the absence of the σ^X mutant was a consequence

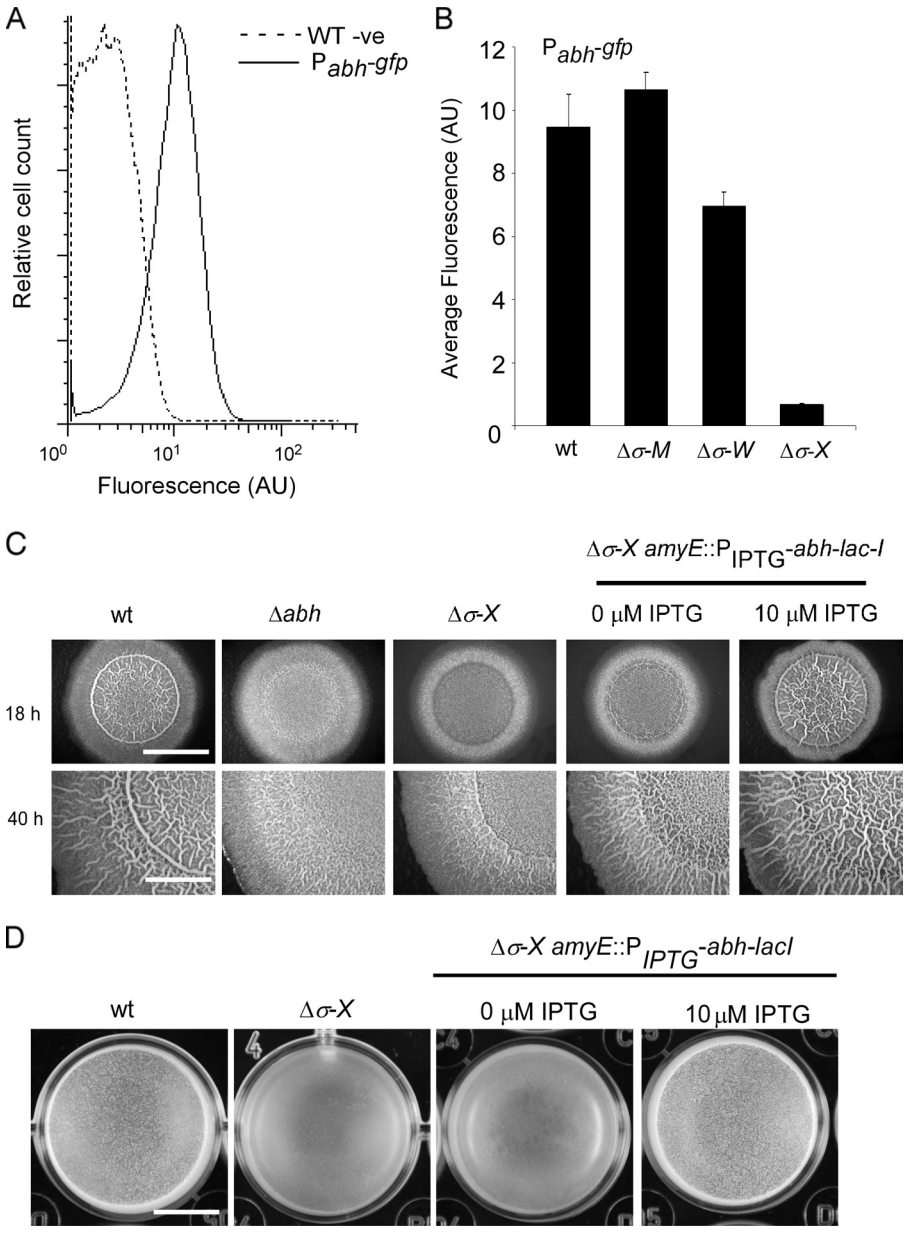

FIG. 2. σ^X activates *abh* expression. (A) Expression of P_{abh}-*gfp* in the wild-type strain (NRS1917) with the NCIB3610 wild-type strain as a nonfluorescent control. Average fluorescence is shown in arbitrary units (AU). WT -ve, wild-type negative control. (B) Expression of P_{abh}-*gfp* was measured in the wild type (wt) (NRS1917), σ^M mutant (Δσ-*M*) (NRS2576), σ^W mutant (Δσ-*W*) (NRS2578), and σ^X mutant (Δσ-*X*) (NRS2577). The values show the means plus standard errors of the means (error bars) from at least three independent experiments. In panels A and B, the cells were incubated for 18 h under biofilm formation conditions and analyzed using flow cytometry. (C) Representative images showing biofilm architecture for the wild-type (NCIB3610), Δ*abh* (NRS1900), σ^X mutant (NRS2572), and σ^X mutant + P_{IPTG}-*abh-lacI* (NRS2575) strains after 18 and 40 h of growth at 37°C. Bars, 5 mm. (D) Same as panel C) for the wild-type (NCIB3610), σ^X mutant (NRS2572), and σ^X mutant + P_{IPTG}-*abh-lacI* (NRS2575) strains. Bar, 5 mm.

of reduced *abh* expression, a copy of *abh* was placed under the control of a heterologous promoter and integrated into the *amyE* locus in the σ^X mutant strain (NRS2575). Induction of *abh* transcription with IPTG restored rugose wild-type biofilm architecture to the σ^X mutant and allowed robust pellicle formation (Fig. 2C and D). These results demonstrate that *abh* is the main downstream target of σ^X that is responsible for developing the mature structure of the biofilm formed by *B. subtilis*.

Consistent with our findings, *B. subtilis* biofilm formation has previously been shown to depend on the combined efforts of σ^X, σ^W, and σ^M which have overlapping regulons (36). However, in contrast to our results, the single σ^X mutants were reported to exhibit wild-type biofilm architecture (36). σ^X is known to be required for survival of *B. subtilis* at high incubation temperatures (25); therefore, we tested whether σ^X, and therefore Abh, control of biofilm architecture, was temperature dependent and grew biofilms at 22°C (room temperature)

and 37°C. (Mascher and coworkers [36] used 22°C, while we used 37°C.) The impact of mutating either σ^X or *abh* was reduced with a reduction in the incubation temperature (data not shown). These results indicate that at higher incubation temperatures, σ^X, and therefore Abh, play a more crucial role in controlling the architecture of the biofilm. They also suggest that at lower temperatures, some other unknown factor can compensate for *abh* under these particular environmental conditions.

It is still unclear what stimulates σ^X activity, but activation of σ^X has been shown to be upregulated when genes predicted to be responsible for drug efflux, peptide uptake, sugar metabolism, and antimicrobial production are inactivated (52). These observations suggest that the signal(s) which stimulates σ^X activation may include the export of toxic molecules, presence of cell density signals, and production of antimicrobial compounds. This led to the proposal that σ^X was required for maintaining cell envelope homeostasis (52). Therefore, *B. subtilis* biofilm formation can be activated by Spo0A in response to surfactin (33) but additionally can influenced by an unknown signal controlling σ^X function which may be perturbations of cell envelope homeostasis. The roles of both of these regulatory pathways in controlling biofilm formation in ecological settings remain to be evaluated.

Biofilm matrix production is controlled by Abh. To understand why biofilm architecture was impacted by the absence of Abh, we considered what effect deletion of *abh* would have on the expression of the *yqxM* and *eps* operons. The *yqxM* and *eps* operons are two loci in *B. subtilis* that are critical for the biosynthesis of the extracellular matrix (6). To determine the impact of deleting *abh* on expression, the upstream promoter region for both the *yqxM* and *eps* operons was fused independently to *gfp* and the level of fluorescence was measured using flow cytometry in the presence and absence of *abh*. The *eps* and *yqxM* promoters are bistable and therefore active in only a subpopulation of cells (10, 55). We found that deletion of *abh* did not affect the bistable profile from being established, but we saw that the number of GFP-positive cells was reduced in the absence of *abh* for both promoters (Fig. 3A and B). For the P_{yqxM}-*gfp* construct, the number of GFP-positive cells decreased from 50% of total population after 18 h of incubation to 35% ($P < 0.01$), and for the P_{eps}-*gfp* construct, it went from 68% to 47% ($P < 0.01$) (Fig. 3C). When considering only the active population of cells that produce each matrix component, these data indicate that in a Δ*abh* biofilm, the number of cells initiating transcription of the loci required for matrix production is reduced ca. 33%. We chose to monitor expression after 18 h of incubation, as this time point corresponds to the peak in expression from these promoters under static incubation conditions (55; our unpublished findings). Ectopic expression of *abh* under the control of its native promoter in the Δ*abh* strain negated the impact of deleting *abh* and increased the number of cells expressing the P_{yqxM}-*gfp* and P_{eps}-*gfp* fusion (Fig. 3C). Consistent with these findings, it has been shown in strain ATCC 6051 that deletion of *abh* inhibits the formation of cell clusters which have been shown to depend on the biosynthesis of the extracellular matrix (29). Therefore, we conclude that the altered biofilm architecture produced by the Δ*abh* strain is a result of a reduction in the number of cells producing the biofilm matrix components, namely, TasA and the exopolysaccharide.

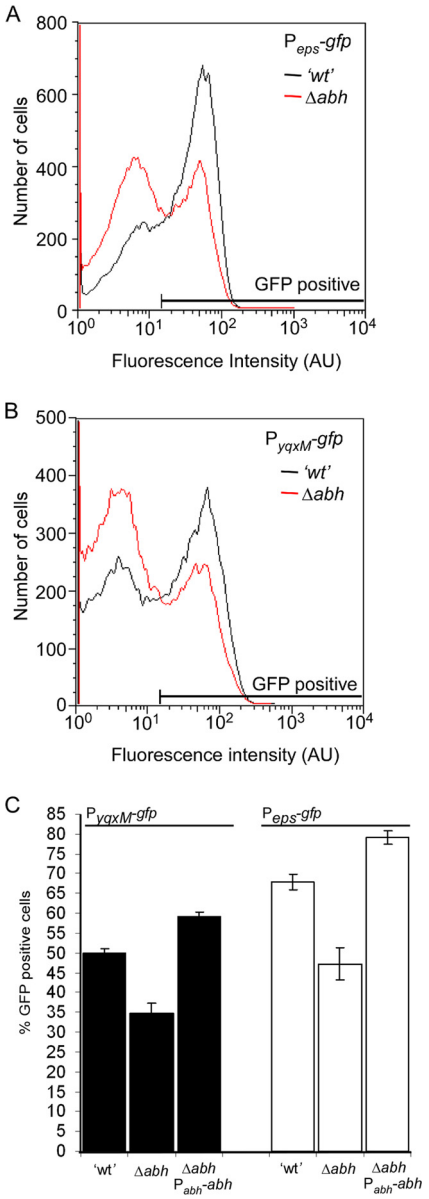

FIG. 3. Abh activates transcription of the loci required for the synthesis of the biofilm matrix. P*epsA-gfp* (A) and P*yqxM-gfp* (B) expression was measured after 18 h of incubation under biofilm formation conditions using flow cytometry. Representative graphs of wild-type ('wt') (NRS2242 [P*eps-gfp*] and NRS2394 [P*yqxM-gfp*]) and Δ*abh* (NRS2547 [P*eps-gfp*] and NRS2549 [P*yqxM-gfp*]) are shown. Fluorescence intensity is shown in arbitrary units (AU). (C) The average number of wild-type (NRS2242 [P*eps-gfp*] and NRS2394 [P*yqxM-gfp*]), Δ*abh* (NRS2547 [P*eps-gfp*] and NRS2549 [P*yqxM-gfp*]) and Δ*abh* + P_{abh}-*abh* (NRS2556 [P*eps-gfp*] and NRS2557 [P*yqxM-gfp*]) cells that were determined to be GFP positive are plotted. The values show the means and standard errors of the means (error bars) from at least three independent experiments.

Abh activates *slrR* transcription. Although it is clear that Abh promotes the formation of an architecturally complex biofilm (Fig. 1) by controlling transcription of the *eps* and *yqxM* operons (Fig. 3), the mechanism by which expression of the *eps*

and *yqxM* operons was controlled by Abh remained unknown. As part of an independent study, we conducted microarray analysis to identify genes regulated by Abh (to be published separately). During data analysis, it was noted that transcription of *slrR* was reduced in the absence of *abh* (1.8-fold ± 0.03-fold reduction [mean ± standard error of the mean]; $n = 3$; $P = 0.05$). Past data demonstrated that SlrR is an activator of biofilm formation which positively activates transcription from the promoter of the *yqxM* operon in *B. subtilis* strain NCIB3610 and positively influences transcription from the promoters of the *yqxM* and *eps* operons in *B. subtilis* strain ATCC 6051 (12, 31). Therefore, we proposed that Abh activation of *slrR* transcription could provide the link between Abh and its role in controlling biofilm architecture. To confirm whether Abh was an activator of *slrR* expression, the *slrR* promoter region (as specified by Chu et al. [12]) was fused to *gfp* and introduced into the *sacA* locus on the chromosome. Fluorescence generated by the P_{slrR}-*gfp* construct was measured using flow cytometry. P_{slrR}-*gfp* expression during biofilm formation was found to be very low in the wild-type strain, which is consistent with previous reports (12). We determined that *slrR* expression exhibited a normal Gaussian distribution pattern, indicating that *slrR* is transcribed uniformly in all cells during biofilm formation (data not shown). It was previously shown that deletion of *sinR* resulted in a ca. 25-fold increase in *slrR* expression (12); therefore, for a positive control, the P_{slrR}-*gfp* expression level was measured during biofilm formation in a Δ*sinIR* strain (NRS2554). Deletion of both *sinI* and *sinR* in combination resulted in an approximately eightfold increase in P_{slrR}-*gfp* expression (data not shown). Additionally, DegU, an activator of biofilm formation (40), has recently been shown not to influence *slrR* transcription (56); therefore, for a negative control, we deleted *degU* and measured the level of P_{slrR}-*gfp* expression. Consistent with previous findings (56), no difference in the level of expression in the absence of *degU* was observed ($P = 0.25$) (Fig. 4). In contrast, and consistent with our DNA microarray analysis, when the P_{slrR}-*gfp* fluorescence was measured in the Δ*abh* strain (NRS2551), a statistically significant reduction in the level of *slrR* transcription was observed (1.5-fold reduction; $P < 0.01$) (Fig. 4). Given that the wild-type levels of *slrR* transcription are very low (12), this is a significant finding. Ectopic expression of *abh* using either the native or inducible promoter returned P_{slrR}-*gfp* expression back to a level that was comparable to that of the wild-type strain, confirming that the reduction in fluorescence was specifically due to the lack of *abh* (Fig. 4). These data indicate that in addition to SinR and AbrB inhibiting *slrR* transcription (12), Abh functions to enhance *slrR* expression.

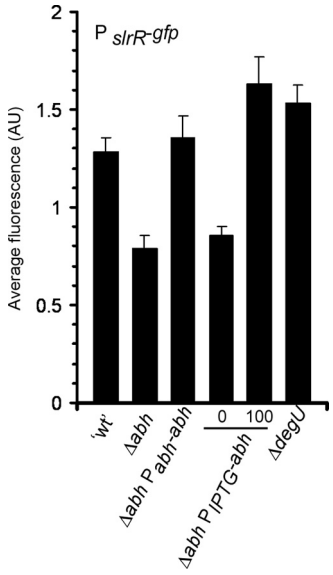

FIG. 4. Abh activates *slrR* expression. Expression of P_{slrR}-*gfp* was measured after 18 h of incubation under biofilm formation conditions at 37°C for the "wild type" ('wt') (NRS2550), Δ*abh* mutant (NRS2551), Δ*abh* P_{abh}-*abh* mutant (NRS2553), Δ*abh* P_{IPTG}-*abh* mutant (NRS2552), and *degU* mutant (NRS2716). Average fluorescence is shown in arbitrary units (AU). The level of IPTG added is shown below the bars (0 for 0 μM IPTG or 100 for 100 μM IPTG). The values show the means plus standard errors of the means (error bars) from at least three independent experiments.

Abh indirectly regulates *slrR* transcription. The data presented so far indicated that Abh influences expression of three loci required for biofilm formation (namely, the *slrR* gene and *eps* and *yqxM* operons) (Fig. 3 and 4). It should be noted that *epsA* and *slrR* are divergently transcribed, and therefore, the promoter regions are contained within the same fragment of intergenic DNA (Fig. 5B). It has been proposed that during control of sublancin production, Abh functions to relieve AbrB-mediated repression of transcription by outcompeting AbrB for shared regulatory binding sites in the promoter region (35). This "molecular displacement" model is unlikely to occur at the *yqxM* promoter, as Abh has not been found to bind to the *yqxM* promoter DNA in vitro (49). However, we wondered whether the molecular displacement model may account for the opposing influence of Abh and AbrB on transcription at the *slrR* and *eps* promoters. An inbuilt requirement for this model was the assumption that AbrB was able to bind to the DNA. While it is recognized that transcription of *eps* and *slrR* is repressed by AbrB, EMSAs using the region between the *eps* operon and the *slrR* gene and purified His-tagged AbrB did not demonstrate any binding interaction in vitro (12). It is our experience that when AbrB is epitope tagged, it is not as efficient at binding DNA as when it is purified unmodified (data not shown). Therefore, we chose to readdress the question of whether AbrB bound to the region between the *eps* operon and the *slrR* gene. To test this, we used EMSA analysis (Fig. 5A). The apparent dissociation constant under the conditions used (room temperature, pH 8, 100 mM KCl) was determined to be 0.65 μM ± 0.1 μM. Binding of AbrB to the region between the *eps* operon and the *slrR* gene was established as cooperative in nature, as less than 20% of AbrB was bound at 0.5 μM but greater than 80% of AbrB was bound at 0.9 μM (Fig. 5A). Having concluded that AbrB interacted directly with the region between the *eps* operon and the *slrR* gene, we used DNA footprinting analysis to test whether Abh could also bind to the DNA region between the *eps* operon and the *slrR* gene, and if so, whether the binding sites overlapped with those for AbrB.

The results of our analysis are shown in Fig. 5C and indicate that Abh does not bind to the region between the *eps* operon and the *slrR* gene. No regions of DNase protection were visible with increasing concentrations of Abh (Fig. 5C, lanes 3, 4 and

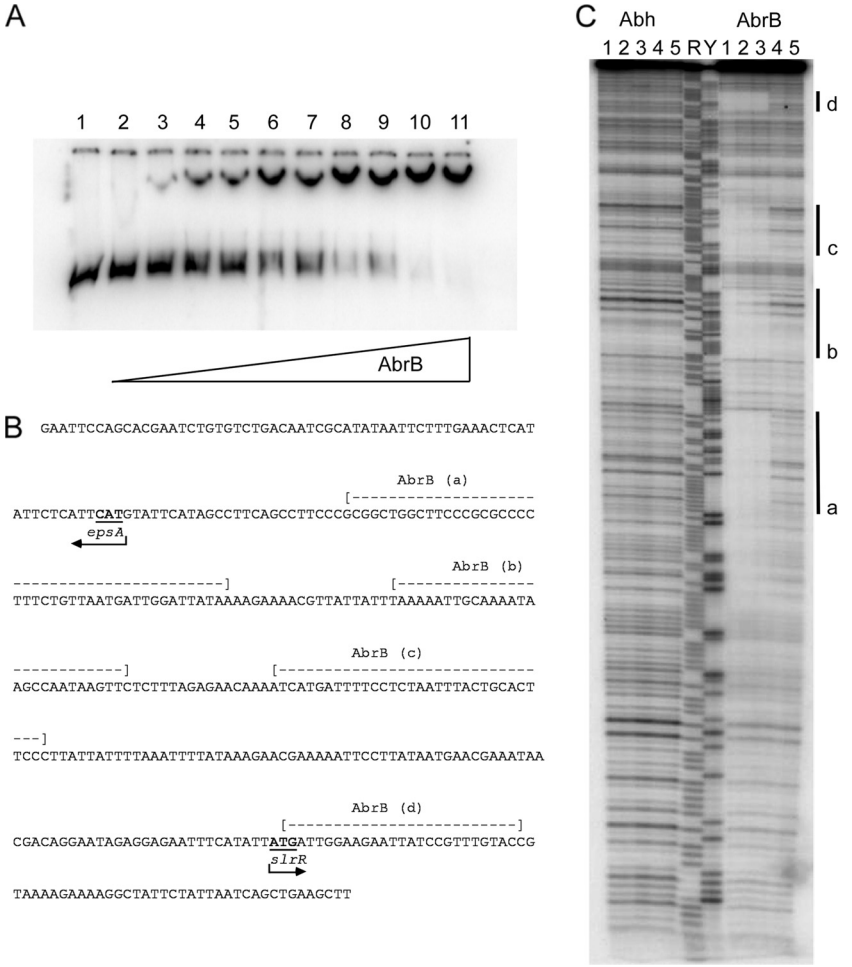

FIG. 5. Abh and AbrB regulate matrix production indirectly and directly, respectively. (A) Electrophoretic mobility shift assays demonstrate that AbrB binds to the region of DNA between the *slrR* gene and the *eps* operon. The concentration of AbrB is as follows: lane 1, 0 μM; lane 2, 0.1 μM; lane 3, 0.3 μM; lane 4, 0.38 μM; lane 5, 0.5 μM; lane 6, 0.6 μM; lane 7, 0.75 μM; lane 8, 0.9 μM; lane 9, 1.0 μM; lane 10, 2.0 μM; lane 11, 3.0 μM. (B) The DNA sequence used in the EMSA and DNA footprinting analysis is provided. The AbrB binding regions are indicated above the nucleotide sequence. The arrowheads indicate the translational start codon for both *epsA* and *slrR*. (C) DNA footprinting analysis of the region between the *slrR* gene and the *eps* operon. The concentrations of Abh and AbrB are as follows: lanes 1 and 2, 0 μM; lane 3, 0.3 μM; lane 4, 3 μM; lane 5, 30 μM. The four AbrB binding regions are labeled a to d and are highlighted by the thick black line. The nucleotides covered by the binding are shown in panel B. Maxam-Gilbert purine and pyrimidine sequence ladders are shown in lane R and lane Y, respectively, for reference.

5). The purified Abh used in the experiments was confirmed to be active using a DNA target (C47) previously shown to bind purified Abh in vitro (data not shown) (4). In contrast, the DNA footprinting analysis supports the EMSA analysis and indicates that AbrB binds to the region between the *eps* operon and the *slrR* gene at four distinct regions (Fig. 5B and C, lanes 3, 4, and 5). These data clearly demonstrate that AbrB repression of *eps* and *slrR* transcription is directly mediated. The fact that Abh was found not to bind to either the region between the *eps* operon and the *slrR* gene (Fig. 5C) or to the promoter of the *yqxM* operon (49) indicates that Abh activation of matrix production is achieved through an indirect mechanism and therefore is different from that proposed for the regulation of sublancin production (35, 49).

Abh controls matrix production through regulation of *slrR* transcription. There is conflicting evidence in the literature as to whether SlrR activates transcription from only the promoter of the *yqxM* operon or whether SlrR also activates expression from the promoter of the *eps* operon (compare reference 12 to reference 31). Our data demonstrate that deletion of *abh* results in a reduction in the number of cells that activate transcription from the operons required for matrix production (*eps* and *yqxM*) (Fig. 3), as well as demonstrating a reduction in the level of *slrR* transcription (Fig. 4). The simplest model that could be proposed to explain our findings in the absence of any direct interaction is that Abh indirectly influences *slrR* transcription (Fig. 4 and 5) and SlrR subsequently controls *eps* and *yqxM* transcription. Integral to this model is SlrR activation of *eps* expression. Therefore, it was necessary to clarify whether or not SlrR activated transcription from the *eps* promoter.

To determine whether SlrR influenced transcription of the *eps* operon, we chose to use flow cytometry with strains containing the P*eps-gfp* reporter fusion. This allowed us to examine expression at the single-cell level under biofilm formation conditions. We used strains that contained the P*yqxM-gfp* fusion as a positive control (12, 31). Strains were constructed that

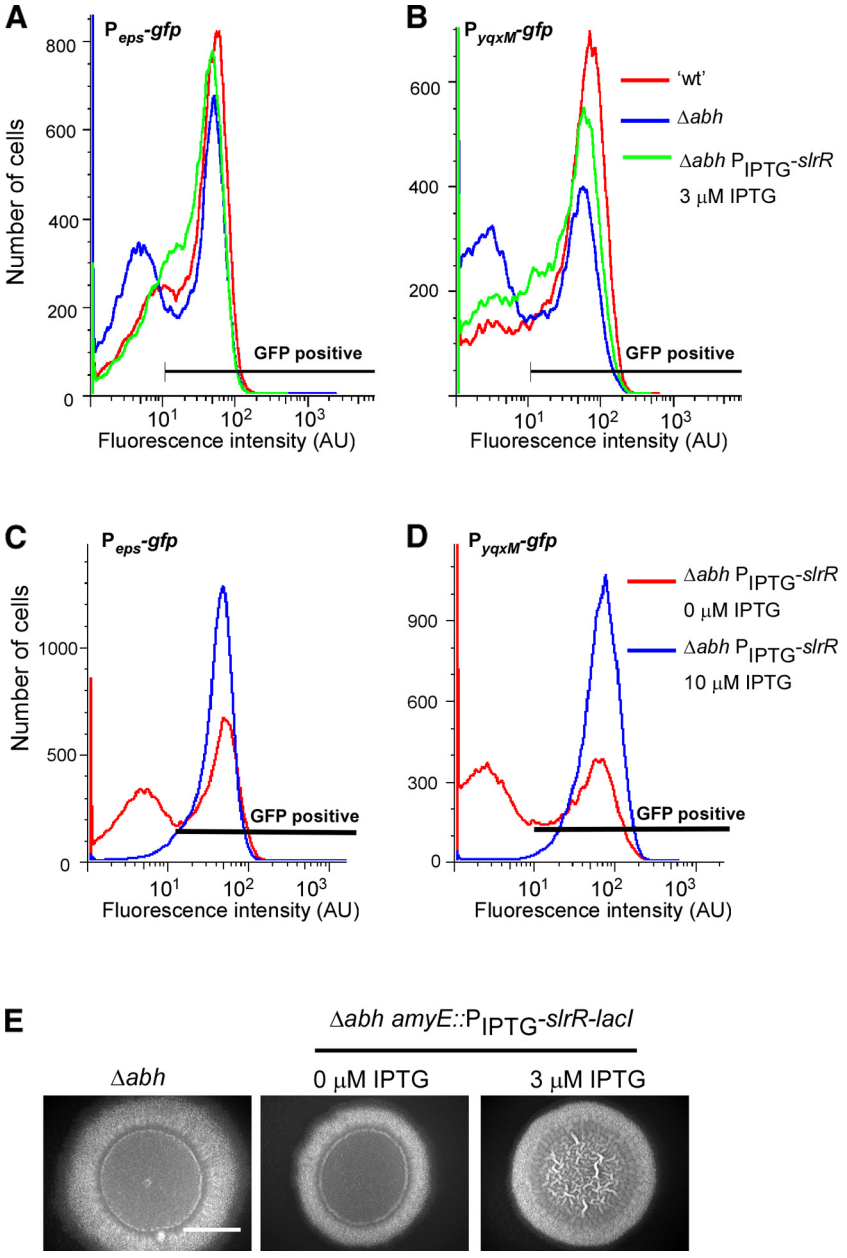

FIG. 6. Abh activates matrix production by activation of *slrR*. P*epsA-gfp* (A and C) and P*yqxM-gfp* (B and D) expression was measured after 18 h of incubation under biofilm formation conditions using flow cytometry. Representative graphs of wild type ('wt') (NRS2242 [P*eps-gfp*] and NRS2394 [P*yqxM-gfp*]) and Δ*abh* mutants (NRS2547 [P*eps-gfp*] and NRS2549 [P*yqxM-gfp*]) and Δ*abh amyE*::P_{IPTG}-*slrR* mutants (NRS2605 [P*eps-gfp*] and NRS2606 [P*yqxM-gfp*]) are shown. The IPTG concentrations are indicated in the panels. Fluorescence intensity is shown in arbitrary units (AU). (E) Representative images showing biofilm architecture for the Δ*abh* (NRS1900) and Δ*abh* + P_{IPTG}-*slrR-lacI* (NRS1966) strains after 18 h at 37°C. The IPTG concentrations are indicated. Bar, 5 mm.

contained the Δ*abh* mutation so that we could simultaneously determine whether the decrease in *slrR* transcription seen in the Δ*abh* strain (Fig. 4) accounted for the reduced number of cells that expressed the operons required for matrix production (Fig. 3). The level of *slrR* transcription was artificially modulated by placing *slrR* under the control of the IPTG-inducible promoter at the *amyE* locus in strains NRS2605 (Δ*abh* P_{IPTG}-*slrR-lacI* P*eps-gfp*) and NRS2606 (Δ*abh* P_{IPTG}-*slrR-lacI* P*yqxM-gfp*) (Table 1). The number of cells expressing the matrix-encoding operons was calculated using flow cytometry after growth in the presence of 0 μM, 3 μM, and 10 μM IPTG for 18 h. The wild-type and Δ*abh* strains served as controls (Fig. 6A and B). The data show that for both reporter fusions, the addition of 3 μM IPTG resulted in an increase in the number of cells expressing the operons required for matrix production. This was concluded as the profile observed by flow cytometry was comparable to that seen for the wild type (Fig. 6A and B). In contrast, at higher concentrations of IPTG (e.g., 10 μM and 100 μM IPTG [data not shown]), it was found that all of the cells in the biofilm activated transcription from the promoters

of the *eps* and *yqxM* operons (Fig. 6C and D). These findings demonstrate that SlrR either directly or indirectly controls transcription from the *eps* operon and that small changes in the level of SlrR have a large influence on transcription.

Induction of P_{IPTG}-*slrR-lacI* with 3 μM IPTG in the Δ*abh* mutant restored the transcription profile with respect to both the P*eps* and P*yqxM* promoters back to the wild-type profile (Fig. 6A and B). Consistent with this, a low level of *slrR* induction was found to compensate for the Δ*abh* mutation with respect to biofilm architecture. This was evident when *slrR* was induced with 3 μM IPTG, which restored the complex "vein"-like structures to the colony formed by the Δ*abh* strain after 18 h of growth (Fig. 6E). (This was the time point at which matrix expression was assayed.) These findings confirm that matrix production is activated by Abh-mediated regulation of *slrR* transcription. Additionally, the data demonstrate that under biofilm-forming conditions, SlrR activates expression of both of the operons required for the biosynthesis of the protein (TasA) and polysaccharide components of the biofilm matrix.

Concluding remarks. We have shown that Abh positively regulates biofilm architecture and that *abh* transcription is controlled in a σ^X-dependent manner under biofilm formation conditions in response to an unidentified signal. This suggests that upon release of σ^X into the cytoplasm by RsiX, its membrane-bound antagonist (25), σ^X can associate with the RNA polymerase core enzyme to activate *abh* transcription. We predict that Abh is the sole (or at least the major) downstream target of σ^X responsible for controlling biofilm architecture, since ectopic expression of *abh* in the σ^X mutant strain fully complements the σ^X mutant biofilm defect (Fig. 2C). The intramembrane-cleaving protease RasP has recently been shown to activate biofilm formation by *B. subtilis* (23). RasP is one of a number of proteases that is required to degrade RsiW, the σ^W anti-sigma factor. Degradation of RsiW results in the release of σ^W from the membrane and allows the genes in the σ^W regulon to be activated (47). It remains to be tested whether RasP also controls induction of σ^X, but if it does, this would be consistent with the biofilm phenotype of both the *rasP* and σ^X mutant strains (23).

The role for Abh in controlling biofilm architecture is the opposite of its paralogue AbrB which inhibits biofilm formation by binding to the promoter regions and blocking transcription from multiple promoters (34, 41, 54) (Fig. 5). We demonstrate that Abh controls the expression of three AbrB-repressed targets, the *slrR* gene and the *eps* and *yqxM* operons that are required for biofilm formation (Fig. 4 and 5A). We eliminate the possibility that Abh positively regulates biofilm architecture by counteracting AbrB-mediated repression exerted on the operons required for biosynthesis of the extracellular matrix since DNA footprinting analysis revealed that Abh does not bind directly to the region between the *eps* operon and the *slrR* gene (Fig. 5). This is consistent with previous findings indicating that Abh regulation of expression of the *yqxM* operon is indirectly mediated (49). Taken together with our findings that low levels of induction of *slrR* in the Δ*abh* strain can complement matrix production and biofilm architecture, the data suggest that Abh exerts its regulatory control solely through indirect activation of *slrR* transcription.

There are several open-ended questions that arise as a consequence of this work. Starting at the top of the regulatory cascade, the environmental signal that activates σ^X has not been identified. Our data indicate that under specific environmental conditions the σ^X pathway will provide a route to stimulate biofilm formation. Downstream of σ^X, it remains to be determined how Abh influences *slrR* transcription as we know from DNA footprinting analysis that this is unlikely to be directly mediated. With respect to SlrR, it is unknown how SlrR activates transcription from the promoter of the *eps* operon, as the *eps* promoter region lacks the proposed SlrR binding site (12). Additionally, it is unknown why overexpression of *slrR* results in activation of *eps* and *yqxM* transcription in all of the cells in the biofilm. These findings indicate that SlrR is somehow capable of overriding the influence of SinR- and AbrB-mediated repression. It is also interesting to note that the regulatory network that controls *slrR* expression described by Kobayashi (31) is repressed by YwcC, a member of the TetR-like repressor family of transcriptional regulators (45). The TetR family of regulators are known to respond to antimicrobial agents that could also trigger σ^X activity (45). Thus, *slrR* transcription may be activated by two separate pathways which are activated upon sensing of antimicrobial agents that disrupt cell envelope homeostasis. In summary, our findings indicate that the production of the biofilm matrix is influenced by an as yet unidentified environmental stimulus that regulates the activity of the ECF σ-factor, σ^X. These findings highlight the extensive ways by which *B. subtilis* regulates the transcription of the operons required for biofilm formation.

ACKNOWLEDGMENTS

This work was supported by the Biotechnology and Biological Sciences Research Council (grant numbers BB/C520404/1 and BB/E001572/1).

We acknowledge Adel Ibrahim from the College of Life Sciences cloning service for constructing pNW407. We thank Kazuo Kobayashi and Beth Lazazzera for helpful discussions, Adam Ostrowski for pNW602, and John Helmann for generously sharing strains with us.

REFERENCES

1. **Bai, U., I. Mandic-Mulec, and I. Smith.** 1993. SinI modulates the activity of SinR, a developmental switch protein of *Bacillus subtilis*, by protein-protein interaction. Genes Dev. **7:**139–148.
2. **Banse, A. V., A. Chastanet, L. Rahn-Lee, E. C. Hobbs, and R. Losick.** 2008. Parallel pathways of repression and antirepression governing the transition to stationary phase in *Bacillus subtilis*. Proc. Natl. Acad. Sci. USA **105:**15547–15552.
3. **Blair, K. M., L. Turner, J. T. Winkelman, H. C. Berg, and D. B. Kearns.** 2008. A molecular clutch disables flagella in the *Bacillus subtilis* biofilm. Science **320:**1636–1638.
4. **Bobay, B. G., A. Andreeva, G. A. Mueller, J. Cavanagh, and A. G. Murzin.** 2005. Revised structure of the AbrB N-terminal domain unifies a diverse superfamily of putative DNA-binding proteins. FEBS Lett. **579:**5669–5674.
5. **Bobay, B. G., G. A. Mueller, R. J. Thompson, A. G. Murzin, R. A. Venters, M. A. Strauch, and J. Cavanagh.** 2006. NMR structure of AbhN and comparison with AbrBN: first insights into the DNA binding promiscuity and specificity of AbrB-like transition state regulator proteins. J. Biol. Chem. **281:**21399–21409.
6. **Branda, S. S., F. Chu, D. B. Kearns, R. Losick, and R. Kolter.** 2006. A major protein component of the *Bacillus subtilis* biofilm matrix. Mol. Microbiol. **59:**1229–1238.
7. **Branda, S. S., J. E. Gonzalez-Pastor, S. Ben-Yehuda, R. Losick, and R. Kolter.** 2001. Fruiting body formation by *Bacillus subtilis*. Proc. Natl. Acad. Sci. USA **98:**11621–11626.
8. **Britton, R. A., P. Eichenberger, J. E. Gonzalez-Pastor, P. Fawcett, R. Monson, R. Losick, and A. D. Grossman.** 2002. Genome-wide analysis of the stationary-phase sigma factor (sigma-H) regulon of *Bacillus subtilis*. J. Bacteriol. **184:**4881–4890.
9. **Burbulys, D., K. A. Trach, and J. A. Hoch.** 1991. Initiation of sporulation in *B. subtilis* is controlled by a multicomponent phosphorelay. Cell **64:**545–552.
10. **Chai, Y., F. Chu, R. Kolter, and R. Losick.** 2008. Bistability and biofilm formation in *Bacillus subtilis*. Mol. Microbiol. **67:**254–263.

11. **Chu, F., D. B. Kearns, S. S. Branda, R. Kolter, and R. Losick.** 2006. Targets of the master regulator of biofilm formation in *Bacillus subtilis*. Mol. Microbiol. **59:**1216–1228.
12. **Chu, F., D. B. Kearns, A. McLoon, Y. Chai, R. Kolter, and R. Losick.** 2008. A novel regulatory protein governing biofilm formation in *Bacillus subtilis*. Mol. Microbiol. **68:**1117–1127.
13. **Dahl, M. K., T. Msadek, F. Kunst, and G. Rapoport.** 1992. The phosphorylation state of the DegU response regulator acts as a molecular switch allowing either degradative enzyme synthesis or expression of genetic competence in *Bacillus subtilis*. J. Biol. Chem. **267:**14509–14514.
14. **Eiamphungporn, W., and J. D. Helmann.** 2008. The *Bacillus subtilis* σ^M regulon and its contribution to cell envelope stress responses. Mol. Microbiol. **67:**830–848.
15. **Fujita, M., J. E. Gonzalez-Pastor, and R. Losick.** 2005. High- and low-threshold genes in the Spo0A regulon of *Bacillus subtilis*. J. Bacteriol. **187:** 1357–1368.
16. **Gonzalez-Pastor, J. E., E. C. Hobbs, and R. Losick.** 2003. Cannibalism by sporulating bacteria. Science **301:**510–513.
17. **Grossman, A. D.** 1995. Genetic networks controlling the initiation of sporulation and the development of genetic competence in *Bacillus subtilis*. Annu. Rev. Genet. **29:**477–508.
18. **Guerout-Fleury, A. M., N. Frandsen, and P. Stragier.** 1996. Plasmids for ectopic integration in *Bacillus subtilis*. Gene **180:**57–61.
19. **Hamoen, L. W., G. Venema, and O. P. Kuipers.** 2003. Controlling competence in *Bacillus subtilis*: shared use of regulators. Microbiology **149:**9–17.
20. **Hamon, M. A., and B. A. Lazazzera.** 2001. The sporulation transcription factor Spo0A is required for biofilm development in *Bacillus subtilis*. Mol. Microbiol. **42:**1199–1209.
21. **Hamon, M. A., N. R. Stanley, R. A. Britton, A. D. Grossman, and B. A. Lazazzera.** 2004. Identification of AbrB-regulated genes involved in biofilm formation by *Bacillus subtilis*. Mol. Microbiol. **52:**847–860.
22. **Harwood, C. R., and S. M. Cutting.** 1990. Molecular biological methods for *Bacillus*. John Wiley & Sons Ltd., Chichester, England.
23. **Heinrich, J., T. Lunden, V. P. Kontinen, and T. Wiegert.** 2008. The *Bacillus subtilis* ABC transporter EcsAB influences intramembrane proteolysis through RasP. Microbiology **154:**1989–1997.
24. **Helmann, J. D.** 2002. The extracytoplasmic function (ECF) sigma factors. Adv. Microb. Physiol. **46:**47–110.
25. **Huang, X., A. Decatur, A. Sorokin, and J. D. Helmann.** 1997. The *Bacillus subtilis* σ^X protein is an extracytoplasmic function sigma factor contributing to survival at high temperature. J. Bacteriol. **179:**2915–2921.
26. **Huang, X., K. L. Fredrick, and J. D. Helmann.** 1998. Promoter recognition by *Bacillus subtilis* σ^W: autoregulation and partial overlap with the σ^X regulon. J. Bacteriol. **180:**3765–3770.
27. **Huang, X., and J. D. Helmann.** 1998. Identification of target promoters for the *Bacillus subtilis* sigma X factor using a consensus-directed search. J. Mol. Biol. **279:**165–173.
28. **Kearns, D. B., F. Chu, S. S. Branda, R. Kolter, and R. Losick.** 2005. A master regulator for biofilm formation by *Bacillus subtilis*. Mol. Microbiol. **55:**739–749.
29. **Kobayashi, K.** 2007. *Bacillus subtilis* pellicle formation proceeds through genetically defined morphological changes. J. Bacteriol. **189:**4920–4931.
30. **Kobayashi, K.** 2007. Gradual activation of the response regulator DegU controls serial expression of genes for flagellum formation and biofilm formation in *Bacillus subtilis*. Mol. Microbiol. **66:**395–409.
31. **Kobayashi, K.** 2008. SlrR/SlrA control the initiation of biofilm formation in *Bacillus subtilis*. Mol. Microbiol. **69:**1399–1410.
32. **Kunst, F., N. Ogasawara, I. Moszer, A. M. Albertini, G. Alloni, V. Azevedo, M. G. Bertero, P. Bessieres, A. Bolotin, S. Borchert, R. Borriss, L. Boursier, A. Brans, M. Braun, S. C. Brignell, S. Bron, S. Brouillet, C. V. Bruschi, B. Caldwell, V. Capuano, N. M. Carter, S. K. Choi, J. J. Codani, I. F. Connerton, A. Danchin, et al.** 1997. The complete genome sequence of the gram-positive bacterium *Bacillus subtilis*. Nature **390:**249–256.
33. **Lopez, D., M. A. Fischbach, F. Chu, R. Losick, and R. Kolter.** 2009. Structurally diverse natural products that cause potassium leakage trigger multicellularity in *Bacillus subtilis*. Proc. Natl. Acad. Sci. USA **106:**280–285.
34. **Lopez, D., H. Vlamakis, and R. Kolter.** 2009. Generation of multiple cell types in *Bacillus subtilis*. FEMS Microbiol. Rev. **33:**152–163.
35. **Luo, Y., and J. D. Helmann.** 2009. Extracytoplasmic function σ factors with overlapping promoter specificity regulate sublancin production in *Bacillus subtilis*. J. Bacteriol. **191:**4951–4958.
36. **Mascher, T., A. B. Hachmann, and J. D. Helmann.** 2007. Regulatory overlap and functional redundancy among *Bacillus subtilis* extracytoplasmic function σ factors. J. Bacteriol. **189:**6919–6927.
37. **Mascher, T., N. G. Margulis, T. Wang, R. W. Ye, and J. D. Helmann.** 2003. Cell wall stress responses in *Bacillus subtilis*: the regulatory network of the bacitracin stimulon. Mol. Microbiol. **50:**1591–1604.
38. **Matsumoto, T., K. Nakanishi, K. Asai, and Y. Sadaie.** 2005. Transcriptional analysis of the ylaABCD operon of *Bacillus subtilis* encoding a sigma factor of extracytoplasmic function family. Genes Genet. Syst. **80:**385–393.
39. **Middleton, R., and A. Hofmeister.** 2004. New shuttle vectors for ectopic insertion of genes into *Bacillus subtilis*. Plasmid **51:**238–245.
40. **Murray, E. J., T. B. Kiley, and N. R. Stanley-Wall.** 2009. A pivotal role for the response regulator DegU in controlling multicellular behaviour. Microbiology **155:**1–8.
41. **Nagórska, K., K. Hinc, M. A. Strauch, and M. Obuchowski.** 2008. Influence of the σ^B stress factor and *yxaB*, the gene for a putative exopolysaccharide synthase under σ^B control, on biofilm formation. J. Bacteriol. **190:**3546–3556.
42. **Perego, M., G. B. Spiegelman, and J. A. Hoch.** 1988. Structure of the gene for the transition state regulator, *abrB*: regulator synthesis is controlled by the *spo0A* sporulation gene in *Bacillus subtilis*. Mol. Microbiol. **2:**689–699.
43. **Piggot, P. J., and D. W. Hilbert.** 2004. Sporulation of *Bacillus subtilis*. Curr. Opin. Microbiol. **7:**579–586.
44. **Quisel, J. D., W. F. Burkholder, and A. D. Grossman.** 2001. In vivo effects of sporulation kinases on mutant Spo0A proteins in *Bacillus subtilis*. J. Bacteriol. **183:**6573–6578.
45. **Ramos, J. L., M. Martinez-Bueno, A. J. Molina-Henares, W. Teran, K. Watanabe, X. Zhang, M. T. Gallegos, R. Brennan, and R. Tobes.** 2005. The TetR family of transcriptional repressors. Microbiol. Mol. Biol. Rev. **69:**326–356.
46. **Robertson, J. B., M. Gocht, M. A. Marahiel, and P. Zuber.** 1989. AbrB, a regulator of gene expression in *Bacillus*, interacts with the transcription initiation regions of a sporulation gene and an antibiotic biosynthesis gene. Proc. Natl. Acad. Sci. USA **86:**8457–8461.
47. **Schobel, S., S. Zellmeier, W. Schumann, and T. Wiegert.** 2004. The *Bacillus subtilis* sigmaW anti-sigma factor RsiW is degraded by intramembrane proteolysis through YluC. Mol. Microbiol. **52:**1091–1105.
48. **Stanley, N. R., R. A. Britton, A. D. Grossman, and B. A. Lazazzera.** 2003. Identification of catabolite repression as a physiological regulator of biofilm formation by *Bacillus subtilis* by use of DNA microarrays. J. Bacteriol. **185:** 1951–1957.
49. **Strauch, M. A., B. G. Bobay, J. Cavanagh, F. Yao, A. Wilson, and Y. Le Breton.** 2007. Abh and AbrB control of *Bacillus subtilis* antimicrobial gene expression. J. Bacteriol. **189:**7720–7732.
50. **Strauch, M. A., G. B. Spiegelman, M. Perego, W. C. Johnson, D. Burbulys, and J. A. Hoch.** 1989. The transition state transcription regulator abrB of *Bacillus subtilis* is a DNA binding protein. EMBO J. **8:**1615–1621.
51. **Strauch, M. A., V. Webb, G. B. Spiegelman, and J. A. Hoch.** 1990. The Spo0A protein of *Bacillus subtilis* is a repressor of the *abrB* gene. Proc. Natl. Acad. Sci. USA **87:**1801–1805.
52. **Turner, M. S., and J. D. Helmann.** 2000. Mutations in multidrug efflux homologs, sugar isomerases, and antimicrobial biosynthesis genes differentially elevate activity of the σ^X and σ^W factors in *Bacillus subtilis*. J. Bacteriol. **182:**5202–5210.
53. **Verhamme, D. T., T. B. Kiley, and N. R. Stanley-Wall.** 2007. DegU coordinates multicellular behaviour exhibited by *Bacillus subtilis*. Mol. Microbiol. **65:**554–568.
54. **Verhamme, D. T., E. J. Murray, and N. R. Stanley-Wall.** 2009. DegU and Spo0A jointly control transcription of two loci required for complex colony development by *Bacillus subtilis*. J. Bacteriol. **191:**100–108.
55. **Vlamakis, H., C. Aguilar, R. Losick, and R. Kolter.** 2008. Control of cell fate by the formation of an architecturally complex bacterial community. Genes Dev. **22:**945–953.
56. **Winkelman, J. T., K. M. Blair, and D. B. Kearns.** 2009. RemA (YlzA) and RemB (YaaB) regulate extracellular matrix operon expression and biofilm formation in *Bacillus subtilis*. J. Bacteriol. **191:**3981–3991.
57. **Xu, K., and M. A. Strauch.** 2001. DNA-binding activity of amino-terminal domains of the *Bacillus subtilis* AbrB protein. J. Bacteriol. **183:**4094–4098.
58. **Yoshimura, M., K. Asai, Y. Sadaie, and H. Yoshikawa.** 2004. Interaction of *Bacillus subtilis* extracytoplasmic function (ECF) sigma factors with the N-terminal regions of their potential anti-sigma factors. Microbiology **150:**591–599.